# Semiconductor Drift Detectors: Applications and New Devices

**A. Castoldi,[1] C. Fiorini,[1] C. Guazzoni,[1]* A. Longoni[1] and L. Strüder[2]**
[1] Politecnico di Milano, Piazza Leonardo da Vinci 32, I-20133 Milan, Italy
[2] MPI Halbleiterlabor, Paul-Gerhardt-Allee 42, D-81245 Munich, Germany

**Recent technological developments and new topology designs have made semiconductor drift detectors ideal devices for high-resolution x-ray spectrometry. In this paper the basic topology of a semiconductor drift detector with on-chip electronics specially designed for x-ray spectrometry is reviewed. These devices have been used for the first time in x-ray and $\gamma$-ray spectroscopy applications. In particular, the results obtained in non-destructive analyses by using a EDXRF spectrometer based on a Peltier cooled semiconductor drift detector and in photodetection of scintillation light are reported. The working principle and the first experimental results for a novel position-sensitive x-ray detector with spectroscopic capability are presented.**

## INTRODUCTION

In the field of x-ray spectrometry, high-energy resolution and low-energy detection capability are basic requirements. The energy resolution of a detection system depends both on the intrinsic resolution of the detector and on the electronic noise of the system. The intrinsic resolution of the detector depends on the statistical fluctuations related to the conversion mechanism and sets a lower limit to the achievable resolution. The noise added by the readout electronics depends both on the detector characteristics (leakage current and output capacitance) and on the characteristics of the front-end electronics. In order to improve the achievable energy resolution, the detector capacitance and the stray capacitances connected to the output node should be minimized. Moreover, the input capacitance of the front-end electronics should be 'matched' to the detector capacitance.

The semiconductor drift detector (SDD), developed by Gatti and Rehak in 1983,[1] is characterized by a low output capacitance (of the order of 100 fF), independent of the active area. The integration of the first stage of the front-end electronics directly on the detector chip allows the designer to reduce the stray capacitances and to satisfy the matching condition. The low output capacitance results in a higher energy resolution at shorter shaping times with respect to conventional *pin* diodes of the same active area.

The basic idea of the SDD is to deplete fully the semiconductor wafer (usually n-type) through a small $n^+$ contact reverse biased with respect to the $p^+$ implants realized on the two surfaces of the detector. The field created by the remaining fixed charges confines the electrons generated by the incident x-ray in a buried potential channel. An electrostatic field parallel to the surface is superimposed to transport the signal charge to the collecting electrode.

The SDD allows one to determine also the position of incidence of ionizing radiation. As the measure of the position of incidence of the radiation is obtained by measuring the drift time of the signal electrons, a reference signal synchronous with the beginning of the drift of the signal electrons is needed. With x-rays this reference signal must be provided by the SDD itself. One way to obtain a reference signal by exploiting the induction of the holes on the field electrodes has been proposed and tested.[2] However in order to have a high spatial resolution a large number of readout channels for the signal induced by the holes is needed. Moreover, a high event-rate capability is limited owing to the possible occurrence of ghost events. To overcome these problems, a novel position-sensitive x-ray detector with spectroscopic capability has been designed and tested. In the new device the pixel structure typical of a charge-coupled device and the fast readout typical of a SDD are combined.

This paper is centered on the activity of the research group at the Politecnico di Milano in the field of drift detectors and applications. First the relevant characteristics of SDD especially designed for x-ray spectrometry and the on-chip electronics are described. This detector has proved to be an ideal device for applications in x-ray and $\gamma$-ray spectroscopy. The first results obtained in these applications are presented. The final section is devoted to the description of the working principle of a novel position-sensitive x-ray detector with spectroscopic capability together with the analysis of the first experimental results.

## SEMICONDUCTOR DRIFT DETECTORS FOR X-RAY SPECTROMETRY

### SDD with on-chip electronics

In Fig. 1 the architecture of an SDD especially designed for x-ray spectrometry (200 eV–20 keV) is shown.[3] The

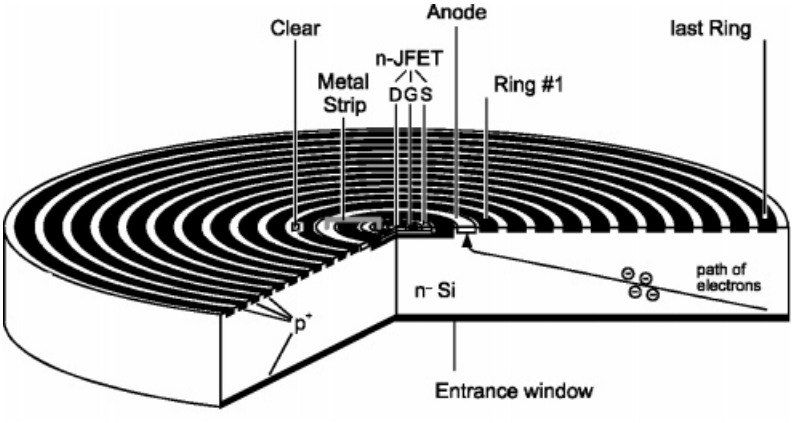


**Figure 1.** Schematic diagram of the SDD with on-chip JFET for x-ray spectrometry.

symmetry of the detector is radial, with a structure composed of $p^+$ concentric rings implanted on the front side of the device. A continuous $p^+$ junction implanted on the rear side of the detector acts as radiation entrance window. With respect to the traditional SDD architecture, where $p^+$ rings were also integrated on the rear side, better soft x-ray detection is achieved by avoiding signal electron trapping in the surface minima under the oxide layer between adjacent rings.[4] This feature, together with careful tailoring of the shallow implantation of the $p^+$ back electrode,[5] allowed us to obtain a detector with an effective 'dead' layer at the entrance window smaller than 150 Å, giving a quantum efficiency higher than 80% at the carbon K$\alpha$ line (277 eV). At high energy, the x-ray detection efficiency, limited by the total thickness of the device (300 μm), is higher than 90% at 10 keV and 50% at 15 keV.

To take full advantage of the intrinsic low output capacitance of the SDD, the input JFET of the 'front-end' electronics has been integrated in the central region of the detector, with the gate connected to the anode by a metal strip (Fig. 1). In this way a correct capacitive matching between the detector and the first stage of amplification is achieved and the stray capacitances of the connections are minimized. This solution has also the advantage of reducing the sensitivity of the detector to the microphonic noise. The integrated transistor is a non-conventional n-channel JFET, designed to be operated on fully depleted high-resistivity silicon.[6]

With an SDD of the type shown in Fig. 1 (active area 3.5 $mm^2$) an energy resolution of 227 eV FWHM at the Mn K$\alpha$ line (5895 eV) was obtained at room temperature with a shaping time of 0.5 μs. The resolution improves to 152 eV FWHM at $-20\,^{\circ}C$ and to 139 eV at $-120\,^{\circ}C$, for a shaping time of 5 μs. The high resolution obtained also at shorter shaping times (162 eV at 250 ns at $-120\,^{\circ}C$) makes the SDD an ideal device for high-rate spectroscopic experiments (EXAFS, x-ray holography) at synchrotron light sources.[7]

### x-ray and $\gamma$-ray spectroscopy applications

The good energy resolution obtained with SDD also at room temperature or at moderately low temperature ($-15\,^{\circ}C$) has recently motivated the development of a small and compact detection module based on an SDD cooled by a Peltier system. The SDD module has already been implemented in electron probe microanalyzers.[8] The module offers a typical energy resolution of better than 160 eV at the Mn K$\alpha$ line at a working temperature of $-15\,^{\circ}C$. With respect to conventionally used Si(Li) detectors, the Peltier-cooled SDD module avoids the use of a liquid nitrogen cryostat and operates at the optimum energy resolution with low values of the shaping time ($<2$ μs).

A portable EDXRF spectrometer based on the SDD module and on a miniaturized x-ray generator (Oxford TF3001, 30 kV, 100 μA) has been developed. In Fig. 2, a photograph of the measurement head of the spectrometer is shown during a measurement on a fresco painting in a church in Bergamo (Italy). The performance of this instrument has been evaluated in several campaigns of measurements performed on works of art directly 'in-the-field'.[9] As an example, in Fig. 3 the fluorescence spectrum measured with the portable spectrometer on a point of a painting attributed to the sixteenth century is reported. From the spectrum, the characteristic lines of Ti and Zn can clearly be identified. Considering that pigments containing Ti and Zn have been introduced only recently (in the last two centuries) in the painting technique, the analysis showed that the painting surface is not original.

In the field of $\gamma$-ray spectrometry, the use of an SDD as a photodetector for the light emitted by scintillating crystals allows the improvement of energy resolution performance. With a first prototype obtained by coupling a CsI(T1) crystal with an SDD with on-chip electronics of 7 $mm^2$ active area, a state-of-the-art energy resolution of 7.49% and 4.34% FWHM (Fig. 4) was obtained at room temperature at 122 and 662 keV, respectively. Moreover, a low energy threshold was reached with the same system: 10 keV at room temperature and $<4$ keV at $0\,^{\circ}C$.[10] According to these results, arrays of SDDs coupled to scintillation crystals are a promising solution for the detection of hard x-rays and $\gamma$-rays in a wide range of applications in astrophysics and nuclear medicine.

## A NOVEL POSITION-SENSING X-RAY DETECTOR WITH SPECTROSCOPIC CAPABILITY

A novel position-sensing x-ray detector with spectroscopic capability, called controlled-drift detector (CDD),

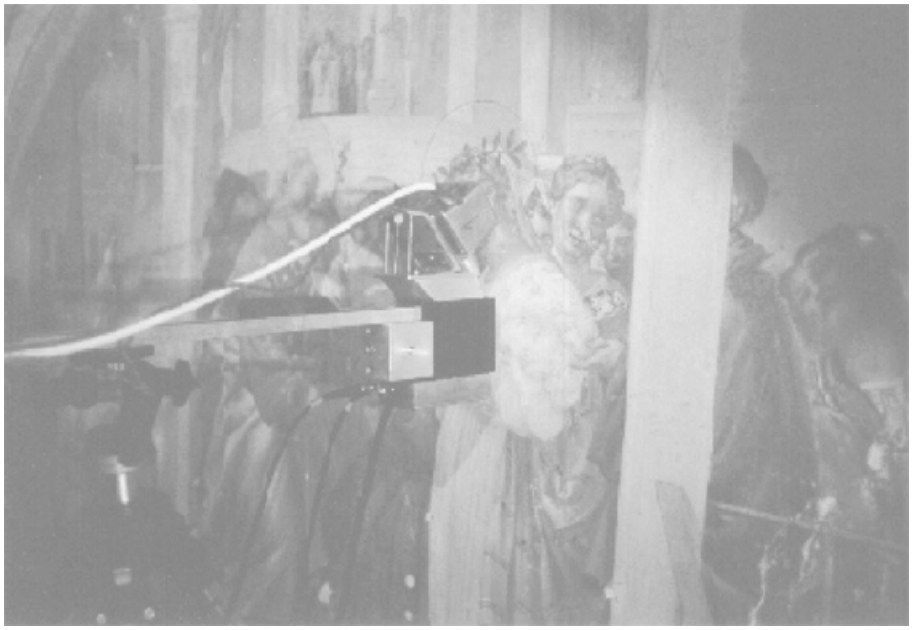

**Figure 2.** A portable EDXRF spectrometer, based on a Peltier-cooled SDD, during a measurement on a fresco painting in a church (Bergamo, Italy).

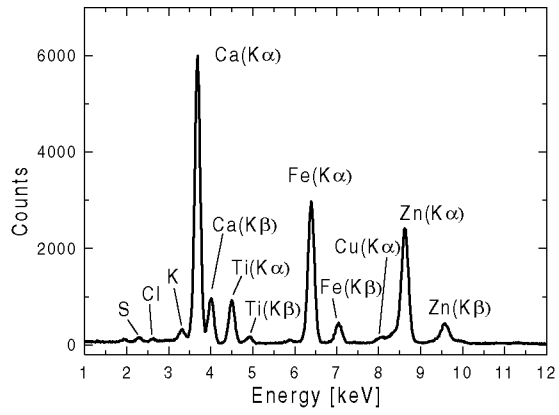


**Figure 3.** X-ray fluorescence spectrum of a point on a painting. The characteristic lines of Ti and Zn can be clearly identified.

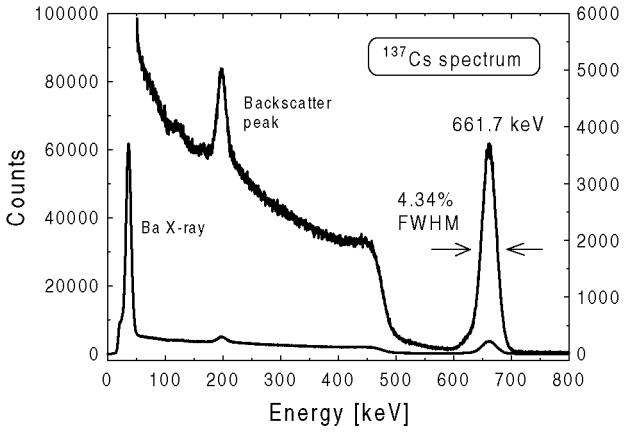


**Figure 4.** Spectrum of the $^{137}$Cs radioactive source measured with the CsI(Tl) SDD detector.

has been recently designed[11] and characterized. The basic idea of the CDD is to join the continuous readout typical of the SDD with the pixel structure typical of the charge-coupled device.

The basic structure of the so-called 'front-driven' CDD is illustrated in Fig. 5. Detailed descriptions of this and other CDD structures are given elsewhere.[11] The detector is operated in the integrate-readout mode. During the integration phase the majority carriers generated by the incident x-rays are rapidly collected from the entire wafer thickness (typically 300 μm) and are stored in a matrix of integration wells, deep in the detector volume. Three on-chip resistive dividers provide a peculiar biasing scheme of the rectifying pn junctions (field strips) of the front side of the detector that is used to create potential wells with linearly increasing negative potentials along a column, going farther from the output electrode. A continuous $p^+$ layer implanted on the rear side of the detector is used as the entrance window for the x-rays. The lateral confinement is achieved by means of channel-stop deep p-implants.[12,13] The pixel size is $180 \times 180$ μm$^2$ and it determines the position resolution achievable with the CDD. The pixel size is given by the period of the perturbation reproduced with the peculiar biasing scheme. A smaller period, leading to smaller pixels, and/or a different shape of the perturbation can also be designed. The smallest pixel size is given by the minimum period required to achieve charge confinement. However, other constraints such as the requirement of a minimum distance of the potential wells from the surface or a limitation in the amplitude of the perturbation that can be applied determines the minimum pixel size in practice. In order to start the read-out phase, the potential barriers that prevent the drift of the charge packet during the integration phase are removed by a small bias change of suitable field strips. The fast transport of the integrated charge packet to the output electrode, placed at the end of each column, is accomplished by means of an electrostatic field, as in the SDD. Full depletion of the detector wafer allows for high x-ray efficiency, small output capacitance and backward illumination.

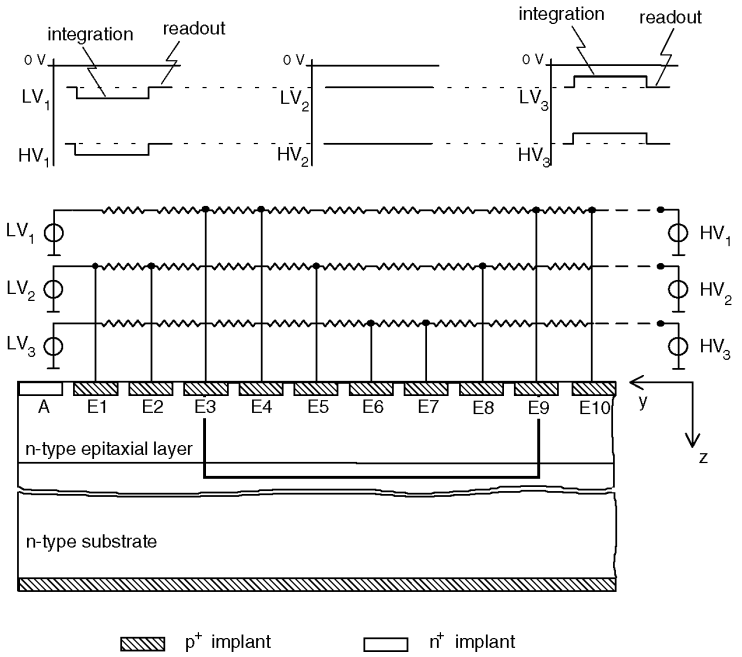


**Figure 5.** Cross-section (not to scale) along the drift coordinate of the controlled-drift detector. The time evolution of the low-voltage (LV) and high-voltage (HV) nodes of the dividers are shown.

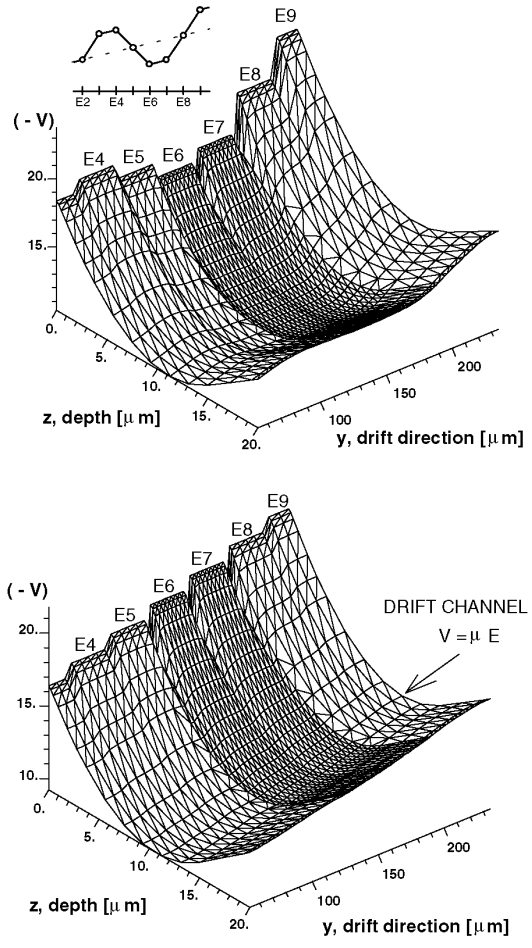


**Figure 6.** Potential energy for the electrons in the detector cross-section shown with a bold line (E3–E9) in Fig. 5. The upper figure refers to the integration phase. The inset shows the biasing scheme of the electrodes of the front side (solid line). The voltage change applied to the drift electrodes is 2 V. The lower figure refers to the readout phase. The applied drift field is 300 V cm$^{-1}$.

Figure 6 shows the simulated electron potential $(-V)$ of the CDD in a cross-section through the center of an output electrode during the integration and the readout phase.

The key feature of the new detector is the high readout speed, proportional to the applied drift field. Figure 7 shows the experimental results of a drift time measurement with the detector biased at 300 V cm$^{-1}$. The measured drift time of the signal electrons is converted in the drifted distance (the calibrating factor is the drift velocity) that identifies the pixel. Negligible drift time non-linearity (less than 1%) ensures safe operation for position sensing with a pixel length of 180 μm. The average drift velocity is 0.35 cm μs$^{-1}$, resulting in a transfer time of 3 μs for a 1 cm long detector. The energy resolution, thanks to the on-chip electronics, is comparable to that obtained with

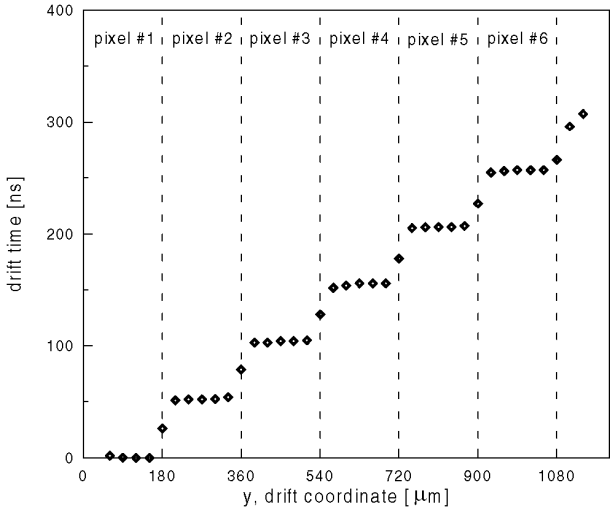


**Figure 7.** Drift time measurements for the CDD biased at 300 V cm$^{-1}$. The incident points of the laser spot are spaced by 30 μm (equal to the p$^+$ strip pitch). The drift time is approximately the same for all the strips within the pixel.

SDDs or with fully depleted pn charge-coupled devices. At room temperature a 205 eV FWHM (the sensitive volume extended over a limited area around the anode and over the whole wafer thickness) at the Mn K$\alpha$ line with a 0.25 μs shaping time has been obtained.

The measured charge handling capacity is $>10^5$ electrons per pixel, ensuring safe operation in the range 1–30 keV.

The controlled-drift detector can provide unambiguous two-dimensional position measurement and high resolution energy spectroscopy with an image timing resolution below 1 ms.

## Acknowledgments

The authors thank E. Gatti, P. Rehak and the staff of the Max Planck Institut für Extraterrestrische Physik Halbleiterlabor (Munich, Germany) for their active and continuous partecipation in the development of drift detectors. Professor Formica is acknowledged for cooperation in the measurements on works of art. This work has been supported by the Italian INFN and MURST.

## REFERENCES

1. E. Gatti and P. Rehak, *Nucl. Instrum. Methods A* **225**, 608 (1984).
2. P. Rehak, J. Walton, E. Gatti, A. Longoni, M. Sampietro, J. Kemmer, H. Dietl, P. Holl, R. Klanner, G. Lutz, A. Wylie and H. Becker, *Nucl. Instrum. Methods A* **248**, 367 (1986).
3. P. Lechner, S. Eckbauer, R. Hartmann, S. Krisch, D. Hauff, R. Richter, H. Soltau, L. Strüder, C. Fiorini, E. Gatti, A. Longoni and M. Sampietro, *Nucl. Instrum. Methods A* **377**, 346 (1996).
4. G. Bertuccio, A. Castoldi, A. Longoni, M. Sampietro and C. Gauthier, *Nucl. Instrum. Methods A* **312**, 613 (1992).
5. R. Hartmann, D. Hauff, P. Lechner, R. Richter, L. Strüder, J. Kemmer, S. Krisch, F. Scholze and G. Ulm, *Nucl. Instrum. Methods A* **377**, 191 (1996).
6. E. Pinotti, H. Bräuninger, N. Findeis, H. Gorke, D. Hauff, P. Holl, J. Kemmer, P. Lechner, G. Lutz, W. Kink, N. Meidinger, G. Metzner, P. Predehl, C. Reppin, L. Strüder, J. Trümper, C. v. Zanthier, E. Kendziorra, R. Staubert, V. Radeka, P. Rehak, G. Bertuccio, E. Gatti, A. Longoni, A. Pullia and M. Sampietro, *Nucl. Instrum. Methods A* **326**, 85 (1993).
7. C. Gauthier, J. Goulon, E. Moguiline, A. Rogalev, P. Lechner, L. Strüder, C. Fiorini, A. Longoni, M. Sampietro, H. Besch, R. Pfitzner, H. Schenk, U. Tafelmeier, A. Walenta, K. Misiakos, S. Kavadias and D. Loukas, *Nucl. Instrum. Methods A* **382**, 524 (1996).
8. C. Fiorini, J. Kemmer, P. Lechner, K. Kromer, M. Rohde and T. Schulein, *Rev. Sci. Instrum.* **68**, 2461 (1997).
9. C. Fiorini and A. Longoni, *Rev. Sci. Instrum.* **69**, 1523 (1997).
10. C. Fiorini, A. Longoni, F. Perotti, C. Labanti, P. Lechner and L. Strüder, *IEEE Trans. Nucl. Sci.* **44**, 2553 (1997).
11. A. Castoldi, C. Guazzoni, E. Gatti, A. Longoni, P. Rehak and L. Strüder, *IEEE Trans. Nucl. Sci.* **44**, 1724 (1997); *USA Eur. Pat. Appl.* 98 830089.3 (1998); *Italy Pat. Appl.* 09 032130 (1998).
12. A. Castoldi, P. Rehak and P. Holl, *Nucl. Instrum. Methods A* **377**, 375 (1996).
13. L. Strüder, H. Bräuninger, M. Meier, P. Predehl, C. Reppin, M. Sterzik, J. Trümper, P. Cattaneo, D. Hauff, G. Lutz, K. F. Schuster, A. Schwarz, E. Kenziorra, A. Staubert, E. Gatti, A. Longoni, M. Sampietro, V. Radeka, P. Rehak, S. Rescia, P. F. Manfredi, W. Buttler, P. Holl, J. Kemmer, U. Prechtel and T. Ziemann, *Nucl. Instrum. Methods A* **288**, 227 (1990).